Cannabis-based medicine reduces multiple pathological processes in AβPP/PS1 mice

Running title: Cannabinoids reduce AD-like phenotype in mice

Ester Aso[a,b*], Alexandre Sánchez-Pla[c,d], Esteban Vegas-Lozano[c], Rafael Maldonado[e], Isidro Ferrer[a,b]

[a]Institut de Neuropatologia, Servei d'Anatomia Patològica, IDIBELL-Hospital Universitari de Bellvitge, Universitat de Barcelona, L'Hospitalet de Llobregat, Spain

[b]CIBERNED, Centro de Investigación Biomédica en Red de Enfermedades Neurodegenerativas, Instituto Carlos III, Spain

[c]Departament d'Estadística, Facultat de Biologia, Universitat de Barcelona, Barcelona, Spain

[d]Statistics and Bioinformatics Unit, Institut de Recerca de l'Hospital Universitari de Vall d'Hebron, Barcelona, Spain

[e]Laboratori de Neurofarmacologia, Departament de Ciències Experimentals i de la Salut, Universitat Pompeu Fabra, Barcelona, Spain

*Corresponding author: Ester Aso, Institut de Neuropatologia, Servei d'Anatomia Patològica, IDIBELL-Hospital Universitari de Bellvitge, C/Feixa Llarga s/n, 08907 L'Hospitalet de Llobregat, Spain. Phone: +34-93-2607452; Fax: +34-93-2607503; E-mail: aso@bellvitgehospital.cat

Abstract

Several recent findings suggest that targeting the endogenous cannabinoid system can be considered as a potential therapeutic approach to treat Alzheimer's disease (AD). The present study supports this hypothesis demonstrating that delta-9-tetrahydrocannabinol (THC) or cannabidiol (CBD) botanical extracts, as well as the combination of both natural cannabinoids, which are the components of an already approved cannabis-based medicine, preserved memory in AβPP/PS1 transgenic mice when chronically administered during the early symptomatic stage. Moreover, THC+CBD reduced learning impairment in AβPP/PS1 mice. A significant decrease in soluble $A\beta_{42}$ peptide levels and a change in plaques composition were also observed in THC+CBD-treated AβPP/PS1 mice, suggesting a cannabinoid-induced reduction in the harmful effect of the most toxic form of the Aβ peptide. Among the mechanisms related with these positive cognitive effects, the anti-inflammatory properties of cannabinoids may also play a relevant role. Here we observed reduced astrogliosis, microgliosis and inflammatory-related molecules in treated AβPP/PS1 mice, which were more marked after treatment with THC+CBD than with either THC or CBD. Moreover, other cannabinoid-induced effects were uncovered by a genome-wide gene expression study. Thus, we have identified the redox protein thioredoxin 2 and the signaling protein Wnt16 as significant substrates for the THC+CBD-induced effects in our AD model. In summary, the present findings show that the combination of THC and CBD exhibits a better therapeutic profile than each cannabis component alone and support the consideration of a cannabis-based medicine as potential therapy against AD.

Keywords: tetrahydrocannabinol, cannabidiol, Alzheimer's disease, animal model, therapy

Introduction

Alzheimer's disease (AD) is the most common neurodegenerative disease associated with dementia in the elderly. While a small proportion of AD cases have a genetic basis, the majority of cases are sporadic with unknown etiology. A consistent feature of the AD brain is the presence of senile plaques composed of pathogenic extracellular deposits of β-amyloid (Aβ), a peptide derived from the aberrant processing of the trans-membrane amyloid precursor protein (APP). Aβ fragments are believed to play a central role in the genesis of the disease resulting in memory loss and behavioral changes. A second pathological hallmark of the disease is hyper-phosphorylation of the microtubule-associated protein tau that forms intracellular neurofibrillary tangles. AD is also associated with neuroinflammation and oxidative stress thus exacerbating neurodegenerative damage [1, 2]. The feeble effectiveness of current therapies against AD highlights the need for urgent development of new agents geared to preventing the disease or curbing its progression.

Targeting the endocannabinoid system offers a multi-faceted approach to the treatment of AD as cannabinoid compounds provide neuroprotection by reducing neuronal damage, neuroinflammation, and oxidative stress, as well as by promoting intrinsic repair mechanisms [3, 4, 5]. Recent studies have demonstrated that chronic stimulation with selective synthetic agonists of CB_1 and CB_2 receptors, the most well-known cannabinoid receptors, reduce cognitive impairment and brain alterations associated with Aβ production, in at least three different animal models of AD [6, 7, 8, 9]. Promising results have also been obtained in a murine model of tauopathy using treatment with natural cannabinoids [10]. Moreover, several *in vitro* and *in vivo* observations support the beneficial effects of CB_1 and CB_2 stimulation in AD models. Thus, the activation of CB_1 receptor *in vitro* preserves neuron viability by reducing Aβ-

induced lysosomal membrane permeability [11] and suppressing pro-apoptotic signaling pathways [12]. CB_2 receptor agonists induce Aβ removal by human macrophages [13] and reduce microglial response to Aβ [7, 14]. In addition, certain cannabinoids are also capable of decreasing tau phosphorylation via CB_1 or CB_2 receptor activation [7, 15, 16].

The aim of the present study was to test the therapeutic properties of the combination of delta-9-tetrahydrocannabinol (THC) and cannabidiol (CBD), two phytocannabinoids produced by the plant *Cannabis sativa* that are known to modulate the endogenous cannabinoid system, in an animal model of AD. The compounds are the two main components of Sativex®, which is a cannabinoid-based medicine already launched in eleven countries (including the UK, Canada, Spain, Italy and Germany), and approved in a further thirteen countries. Sativex® is a well-tolerated medicine prescribed for the treatment of spasticity associated with multiple sclerosis and it is also undergoing development for other therapeutic applications including pain of various origins (i.e. cancer) and Huntington's disease [17, 18], a fact that can facilitate the translation from basic research in AD models to human cases. We have used AβPP/PS1 mice as an animal model because they replicate the most relevant features of AD, including cognitive impairment and several pathological alterations such as Aβ deposition, dystrophic neurites, synaptic failure, mitochondrial dysfunction, and oxidative stress damage [19, 20].

Materials and Methods

Animals

The experiments were carried out in male AβPP/PS1 mice and wild-type littermates aged 6 months (early symptomatic phase) at the outset of the study. The generation of mice expressing the human mutated forms APPswe and PS1dE9 has already been described [19]. Animals were maintained under standard animal housing conditions in a 12-h dark-light cycle with free access to food and water. Mice were randomly assigned to treatment groups and the experiments were conducted under blind experimental conditions. All animal procedures were carried out following the guidelines of the European Communities Council Directive 2010/63/EU and with the approval of the local ethical committees of the University of Barcelona and University Pompeu Fabra.

Pharmacological treatment

THC enriched botanical extract (containing 67.1% THC, 0.3% CBD, 0.9% cannabigerol, 0.9% cannabichromene, and 1.9% other phytocannabinoids) and CBD enriched botanical extract (containing 64.8% CBD, 2.3% THC, 1.1% cannabigerol, 3.0% cannabichromene, and 1.5% other phytocannabinoids) were supplied by GW Pharmaceuticals Ltd (Cambridge, UK). The extracts (THC, 0.75 mg/kg; CBD, 0.75 mg/kg; THC+CBD, 0.75 mg/kg each) were dissolved in 5% ethanol, 5% Tween, and 90% saline, and these mixtures were injected intra-peritoneally (i.p.) in a volume of 10 mL/kg body weight. The human equivalent dose (HED) calculated with the formula for dose translation based on body surface area [20] corresponds to 0.04 mg/kg for each cannabinoid, what is equivalent to the administration of a single Sativex® oromucosal spray (2.8 mg THC + 2.8 mg CBD) in a human being weighting 70 kg, and is lacking of psychoactivity. Animals were treated once a day for 5 weeks with the extracts or the

corresponding vehicle (wild-type, n = 7-11; AβPP/PS1, n = 7-8 per group). After 10 days of washing period, animals were subjected to behavioral evaluation.

Behavioral evaluation of cognitive performance and sample collection

Two-object recognition test: This paradigm was performed in a V-maze (Panlab, Barcelona, Spain) because it improves the exploration time of the animals with respect to a classical open field. On day 1, mice were habituated for 9 min, allowing them to freely explore the apparatus. On the second day, mice were placed for 9 min in the maze, where two identical objects were situated at the end of the arms, and the time that the mice spent exploring each object was recorded. Then, 24 h after the training session, animals were placed again in the V-maze where one of the two familiar objects was replaced by a novel object. The time that the animals spent exploring the two objects was recorded and an object recognition index (RI) was calculated as the difference between the time spent exploring the novel (T_N) and the familiar object (T_F), divided by the total time spent exploring the two objects [$RI=(T_N-T_F)/(T_N+T_F)$]. Animals exhibiting memory impairments revealed a lower object recognition index.

Active avoidance test: After the two-object recognition test, the animals were allowed to rest for 4 days before starting the active avoidance test. Then, the mice were trained to avoid an aversive stimulus associated with the presentation of a conditioned stimulus (CS) in a two-way shuttle box apparatus (Panlab, Barcelona, Spain). The CS was a light (10 W) switched on in the compartment in which the mouse was placed. The CS was received 5 sec before the onset of the unconditioned stimulus (US) and overlapped it for 25 sec. At the end of the 30-sec period, both CS and US were automatically turned off. The US was an electric shock (0.2 mA) continuously applied to the grid of the floor. A conditioned response was recorded when the animal avoided the US by changing from the compartment where it received the CS to the opposite compartment

within the 5 sec period after the onset of the CS. If animals failed to avoid the shock, they could escape it by crossing during the US (25 sec) and this was recorded as unconditioned response. Between each trial session, there was an inter-trial interval of 30 sec. Animals were subjected to five daily 100-trial active avoidance sessions. Each day, the mice were placed in the shuttle box for 10 min before the start of each session to allow them to explore the box. Data are expressed as the total number of conditioned changes, converted to the area under the curve (AUC) using a standard trapezoid method.

At the end of the behavioral testing, the animals were sacrificed by cervical dislocation and their brains rapidly removed from the skull and processed for study. One hemisphere was dissected on ice, immediately frozen, and stored at -80ºC until used for the protein quantification and the gene expression study. The other hemisphere was fixed in 4% paraformaldehyde and processed for immunohistochemistry.

Aβ immunohistochemistry

Fixed tissue samples were embedded in paraffin, and coronal sections, 4 μm thick, were cut with a microtome. Consecutive de-waxed sections were incubated with 98% formic acid (3 min) and then treated with citrate buffer (20 min) to enhance antigenicity. Then endogenous peroxidases were blocked by incubation in 10% methanol-1% H_2O_2 solution (15 min). Sections were blocked with 3% normal horse serum solution and then incubated at 4ºC overnight with the primary antibody against $A\beta_{40}$ (1:100, Merck Millipore, Billerica, MA, USA) or $A\beta_{42}$ (1:50, Merck Millipore). Sections were subsequently rinsed and incubated with biotinylated secondary antibody (Dako), followed by EnVision+ system peroxidase (Dako), and finally with chromogen diaminobenzidine and H_2O_2. Sections were lightly counterstained with hematoxylin. After staining, the sections were dehydrated and cover-slipped for observation under a

Nikon Eclipse E800 microscope (Nikon Imaging Inc., Tokyo, Japan; Objective: 10x). The cortical total $A\beta_{42}$ and $A\beta_{40}$ burden was calculated as the percentage of the area of amyloid deposition in plaques with respect to the total area in 9 representative pictures taken from the cerebral cortex of each animal, corresponding to the main regions where $A\beta_{42}$ and $A\beta_{40}$ deposition is observed in AβPP/PS1 mice. The ratio between $A\beta_{42}$ and $A\beta_{40}$ deposition in each plaque was calculated by comparing the specific staining with each antibody in at least 10 plaques per animal in consecutive sections. Aβ quantification was calculated using the Adobe® Photoshop® CS4 software (Adobe Systems Inc., San Jose, CA, USA), as previously described [20]. All the AβPP/PS1 treated animals were analyzed.

Aβ soluble quantification: enzyme-linked immunosorbent assay (ELISA)

Fresh-frozen mouse brain cortex was homogenized in 4 volumes (wt:vol) of TBS extraction buffer (140 mM NaCl, 3 mM KCl, 25 mM Tris (pH 7.4), 5 mM EDTA, and protease inhibitor cocktail (Roche Molecular Systems, Pleasanton, CA, USA). Homogenate was spun 100,000 g × 1 h, and the supernatant was saved as the soluble fraction for Aβ quantification. $A\beta_{40}$ and $A\beta_{42}$ Human ELISA kits (Invitrogen™ Corporation, Camarillo, CA, USA) were used to quantify the levels of $A\beta_{40}$ and $A\beta_{42}$ peptides in the brain soluble fractions. Quantitative determination was carried out according to the manufacturer's instructions, as previously described [21]. $A\beta_{40}$ and $A\beta_{42}$ levels were normalized to the total amount of protein from each individual sample (BCA method, Thermo Fisher Scientific, Wilmington, DE, USA). Six AβPP/PS1 mice per treatment were analyzed.

Double-labeling immunofluorescence

De-waxed sections were incubated with 98% formic acid (3 min) for Aβ immunofluorescence and then treated with citrate buffer (20 min) to enhance

antigenicity. Sections were stained with a saturated solution of Sudan black B for 30 min (Merck Millipore) to block lipofuscin autofluorescence, then rinsed in 70% ethanol and washed in distilled water. After a blockade with 10% fetal bovine serum (90 min), the sections were incubated at 4ºC overnight with combinations of primary antibodies against Aβ (clone 6F/3D 1:50, Dako), glial fibrillary acidic protein (GFAP; 1:250, Dako) or IBA1 (1:250, Wako, Richmond, VA, USA). After washing, the sections were incubated with Alexa488 or Alexa546 fluorescence secondary antibodies against the corresponding host species (1:400, Molecular Probes, Eugene, OR, USA). Then they were washed and mounted in Immuno-Fluore Mounting medium (ICN Biomedicals, Solon, OH, USA), sealed, dried overnight, and examined with a Nikon Eclipse E800 microscope. The specific GFAP and IBA1 immunostaining density was calculated in reference to the Aβ plaque area in 5 representative pictures taken from the cortex of each animal using the Adobe® Photoshop® CS4 software. Six animals per each group were used for quantifications.

RNA microarray studies

RNA from frozen cortex samples of treated mice was extracted following the instructions of the supplier (Rneasy Mini Kit, Qiagen® GmbH, Hilden, Germany). RNA quality control was tested with the Agilent Bioanalyzer (Agilent Technologies Inc, Santa Clara, CA, USA), and the RNA concentration was evaluated using a NanoDrop™ Spectrophotometer (Thermo Fisher Scientific). A total of 24 samples (6 AβPP/PS1 samples per treatment) were analyzed by microarray hybridization with the GeneChip® Mouse Gene 1.0 ST Array from Affimetrix (Santa Clara, CA, USA). Bioinformatic analysis was performed with a three (+1) step on the probe values to turn them into comparable gene-level expression values: background correction (RMA), normalization (Quantiles), summarization (Median Polish), and transcript-level summarization

(Average). Non-specific filtering was applied to rule out controls, low signal genes, and low variability genes. This pre-processing left 5,606 genes for further study. Functional annotation and biological term enrichment analysis were carried out using the DAVID database (http://david.abcc.ncifcrf.gov/). We used $p < 0.05$ as the cut-off point to determine whether Kyoto Encyclopedia of Genes and Genomes (KEGG) pathways were significantly enriched. Each group was composed by 6 samples.

Quantitative PCR

1 μg total RNA was reverse-transcribed with cDNA synthesized with the High-Capacity cDNA Reverse Transcription kit (Applied Biosystems). Quantification of the mRNA levels was performed in duplicate reactions with gene-specific TaqMan® probes and the TaqMan® Universal PCR Master Mix (Applied Biosystems). House-keeping genes used were Aars, Hprt, and Xpnpep1 [22]. QPCR was performed using the Applied Biosystems 7900HT Fast Real-Time PCR System. Samples were analyzed with the double delta CT (ΔΔCT) method using vehicle-treated AβPP/PS1 samples as control. Six animals per group were analyzed.

Gel electrophoresis and western blotting

Samples of the cerebral cortex were homogenized in RIPA lysis buffer (50mM Tris/HCl buffer, pH 7.4 containing 2mM EDTA, 0.2% Nonidet P-40, 1mM PMSF, protease, and phosphatase inhibitor cocktails, Roche Molecular Systems, USA). The homogenates were centrifuged for 15 min at 13,000 rpm. Protein concentration was determined with the BCA method (Thermo Scientific). Equal amounts of protein (20 μg) for each sample were loaded and separated by electrophoresis on sodium dodecyl sulfate polyacrylamide gel electrophoresis (SDS-PAGE) (10%) gels and transferred onto nitrocellulose membranes (Amersham, Freiburg, Germany). Non-specific bindings were blocked by incubation in 3% albumin in PBS containing 0.2% Tween for 1 h at room temperature.

After washing, membranes were incubated overnight at 4°C with the antibodies against extracellular signal-regulated kinase (ERK)1/2 phospho Thr202/Tyr204 Thr185/Tyr187 (1:1,000, Millipore), ERK1/2 (1:200, Santa Cruz Biotechnology, Dallas, TX, USA), thioredoxin 2 (Txn2, 1:1,000, Proteintech, Chicago, IL, USA) and wingless-related integration site 16 (Wnt16, 1:5,000, GeneTex, Irvine, CA, USA). Protein loading was monitored using an antibody against β-tubulin (1:10,000, Abcam). Membranes were then incubated for 1 h in the appropriate HRP- conjugated secondary antibodies (1:2,000, Dako), and immunocomplexes were revealed by chemiluminescence reagent (ECL, Amersham). Densitometric quantification was carried out with TotalLab v2.01 software (Pharmacia, Sweden). Bands were normalized to β-tubulin. Six animals per group were analyzed.

Statistical analysis

The sample size for experimentation was computed using the Power and Precision software (Biostat, Englewood, NJ, USA), assuming a power of 95% and no missing data. Statistical analysis was performed with the SPSS® Statistics v21.0 software (IBM, New York, NY, USA). The normality of the data was assessed with the Shapiro-Wilk test and as a consequence parametric statistical tests were used for the analysis of all the data in the study. Data were analyzed with two-way ANOVA with genotype and treatment as between factors (memory, AUC, western blotting quantifications) or one-way ANOVA with treatment as between factor (Aß, glia and gene expression quantifications), followed by Tukey's *post hoc* when required. Learning data (conditioned changes) were analyzed by two-way ANOVA with day of training as within factor and genotype as between factor. In all the experiments, the significance level was set at $p < 0.05$.

Results

Natural cannabinoids reduce cognitive deficits in AβPP/PS1 mice

Daily administration of THC (0.75 mg/kg, i.p.), CBD (0.75 mg/kg, i.p.) botanical extracts, or the combination of THC and CBD (0.75 mg/kg each botanical extract, i.p.) during 5 weeks at the early stages of the symptomatic phase (6 months) blunted the memory impairment observed in vehicle-treated AβPP/PS1 mice when compared to wild-type animals on the two-object recognition test (Fig. 1A). Thus, two-way ANOVA revealed a significant treatment effect ($F_{(3, 55)} = 3.57$, $p < 0.05$) and interaction between gentype and treatment ($F_{(3, 55)} = 12.92$, $p < 0.001$), but not genotype effect. Subsequent Tukey's *post hoc* tests revealed that THC ($p < 0.001$), CBD ($p < 0.01$), and THC+CBD ($p < 0.05$) significantly increased the recognition index of AβPP/PS1 mice when compared to vehicle-treated littermates. Chronic exposure to THC botanical extract resulted in reduced memory performance in wild-type mice when compared to vehicle-treated littermates ($p < 0.05$). However, this deleterious effect was not seen in CBD- and THC+CBD-treated wild mice as no impaired memory performance was observed in these animals. No significant difference in the total exploration time during the memory acquisition session or the memory test was observed between groups (Supplementary Table S1), discarding any possible impact of the treatments on the anxiety levels or the activity of mice. Animals exhibited no preference for any object during the acquisition session.

The learning performance of mice was evaluated in the active avoidance test by recording the number of conditioned changes during 5 consecutive training days. The AUC revealed a significant reduction in the learning performance of vehicle- ($p < 0.01$) and CBD-treated ($p < 0.05$) but not in THC- or THC+CBD-treated AβPP/PS1 mice when compared to wild littermates (Fig. 1B). When compared day by day, the number

of conditioned changes achieved by mice was reduced in vehicle-treated AβPP/PS1 mice on day 3 ($p < 0.05$), day 4 ($p < 0.01$) and day 5 ($p < 0.001$; Fig. 1C), in THC-treated on day 5 (Fig. 1D) and in CBD-treated mice on day 3 ($p < 0.05$), day 4 ($p < 0.01$) and day 5 ($p < 0.01$; Fig. 1E) when compared with wild-type animals. In contrast, AβPP/PS1 mice chronically treated with the combination of THC+CBD did not evidence such learning impairment at any day (Fig. 1F). No significant treatment effect was observed respect vehicle group neither in wild-type nor AβPP/PS1 mice. These results demonstrate that the THC+CBD combination rescued AβPP/PS1 learning impairment in the active avoidance paradigm when administered at the beginning of the symptomatic stage. See supplementary Table S2 for statistical details.

The combination of THC and CBD alters Aβ processing in AβPP/PS1 mice

Chronic treatment with THC, CBD, or the combination of both did not significantly modify the total Aβ burden ($F_{(3, 28)} = 0.73$, *N.S.*; Fig. 2B) or the $A\beta_{42}$ ($F_{(3, 22)} = 0.62$, *N.S.*) and $A\beta_{40}$ burden ($F_{(3, 22)} = 0.30$, *N.S.*; Fig. 2C) in the cortex of AβPP/PS1 mice, although there was a tendency to reduced Aβ deposition in THC+CBD-treated animals. Similarly, no significant treatment effect was observed in the total Aβ burden in the hippocampus of AβPP/PS1 mice ($F_{(3, 17)} = 0.83$, *N.S.*; Fig. 2B), which is much lower than the Aβ burden observed in the AβPP/PS1 mice cortex, as expected. However, a significant reduction in $A\beta_{42}$ ($F_{(3, 22)} = 7.88$, $p < 0.001$), but not $A\beta_{40}$ ($F_{(3, 22)} = 1.62$, *N.S*), protein levels was observed in the cortical soluble fraction of THC+CBD-treated AβPP/PS1 mice when compared to vehicle- ($p < 0.01$), THC- ($p < 0.01$) and CBD-treated mice ($p < 0.05$), thus demonstrating a protective effect of the combination of both cannabinoids in AβPP/PS1 animals by reducing the most toxic form of the Aβ peptide (Fig. 2D). The THC+CBD treatment also induced a change ($F_{(3, 23)} = 3.169$, $p < 0.05$) in the composition of Aβ plaques since the ratio $A\beta_{42}/A\beta_{40}$ in each plaque was

increased in treated AβPP/PS1 mice when compared to control group ($p < 0.05$) (Fig. 2E and 2F), suggesting a facilitation of $A\beta_{42}$ deposition that could be related to the reduction of the most toxic $A\beta_{42}$ soluble contents. None of the Aβ forms studied was detectable in wild-type animals, as expected (data not shown).

Natural cannabinoids reduce Aβ deposition-related astrogliosis and cytokine expression in AβPP/PS1 mice

One-way ANOVA revealed a treatment effect in the astrogliosis ($F_{(3, 20)} = 10.86$, $p < 0.001$) and microgliosis ($F_{(3, 20)} = 2.53$, $p < 0.05$) associated to Aβ deposition in AβPP/PS1 mice. A significant reduction in the number of astrocytes around Aβ plaques was observed in mice treated with THC ($p < 0.01$), CBD ($p < 0.001$), or the combination of the two compounds ($p < 0.05$) when compared with vehicle-treated AβPP/PS1 mice, as revealed with quantitative double-labeling immunofluorescence (Fig. 3A and 3B). However, the number of microglial cells associated with Aβ plaques was only significantly reduced by the THC+CBD combination ($p < 0.05$) when compared to vehicle-treated AβPP/PS1 animals (Fig. 3A and 3C). No significant effect on the number of astrocytes and microglial cells was observed in the cortex of treated wild-type mice (data not shown). To assess possible inflammatory changes associated with cannabinoid compounds, we evaluated the expression levels of a panel of cytokine-related genes, which have been previously demonstrated to underlie the inflammatory response in AβPP/PS1 mice and AD brains (López-González et al, *in preparation*), by quantitative PCR. As shown in Table 1, the combination of THC+CBD resulted in a marked modification of the neuroinflammatory responses, which was greater than that resulting from treatment with THC or CBD alone. Reduced inflammatory responses involved a colony stimulating factor receptor (Csf3r), a complement system component (C1qtnf7), a cell surface adhesion protein (Itgb2), Fc receptors (Fcgr1, Fcgr2b), a pro-

inflammatory cytokine (Il6st), a regulator of myeloid cell cycle (Inpp5d), and toll-like receptors (Tlr4, Tlr7). The THC+CBD combination also reduced the expression of two genes related to anti-inflammatory cytokines (Il10rb, Tgfb1).

Natural cannabinoids modify brain gene expression in AβPP/PS1 mice

Additional transcription modifications associated with cannabinoid effects in AβPP/PS1 mice were assessed with RNA microarrays. Natural cannabinoids induced a differential gene expression profile in AβPP/PS1 mice as revealed the heatmap obtained from microarrays studies (Figure 4A). The number of genes significantly modulated in relation to vehicle-treated AβPP/PS1 mice was 142 up-regulated and 142 down-regulated in THC-treated mice; 125 up-regulated and 166 down-regulated in CBD-treated mice; and 187 up-regulated and 136 down-regulated in the THC+CBD group ($p < 0.05$). The Venn's diagram shows that only 23 genes were commonly regulated by the three treatments (Figure 4B). The KEGG enrichment analysis of the results allowed to discover functional-related gene groups significantly modulated by treatments and pointed to degradation processes, immunomodulation, mitochondrial function, and mitogen-activated protein kinase 3 (Mapk3) and wingless-type MMTV integration site family, member 16 (Wnt16) signaling pathways, among others, as relevant molecular mechanisms underlying the effects of natural cannabinoids in AβPP/PS1 transgenic mice (Supplementary Table S3). Eight candidate genes were chosen for validation on the basis of their potential functional relevance and their high-fold change in treated AβPP/PS1 mice. The statistical analysis of the quantitative PCR resulted in: adenylate cyclase 3 (Adcy3; $F_{(3, 20)} = 1.54$, *N.S.*), cytochrome c oxidase subunit VIIc (Cox7c; $F_{(3, 20)} = 2.30$, *N.S.*), Mapk3 ($F_{(3, 20)} = 5.76$, $p < 0.01$), nitric oxide synthase 1 (Nos1; $F_{(3, 20)} = 3.76$, $p < 0.05$), proteasome subunit, beta type, 2 (Psmb2; $F_{(3, 20)} = 3.37$, $p < 0.05$), thioredoxin 2 (Txn2; $F_{(3, 20)} = 5.08$, $p < 0.01$), ubiquitin (Ubb; $F_{(3, 20)} = 3.182$, $p < 0.05$)

and Wnt16 ($F_{(3, 20)}$ = 2.22, p < 0.05). Thus, a Mapk3, Psmb2, Txn2, and Wnt16 decrease was validated in THC+CBD-treated mice (Fig. 4C). Decrease expression of Nos1 and Ubb was observed by quantitative PCR in THC+CBD, which was in contrast with the increase found in RNA microarray. Finally, Adcy3 and Cox7c modifications seen in microarrays were not validated with PCR.

Natural cannabinoids modulate MAPK3, Txn2 and Wnt16 protein levels in AβPP/PS1 mice

We assessed the correlation between the cannabinoid-induced alteration of Mapk3, Txn2, and Wnt16 gene expression and the levels of the proteins coded by those genes using western blotting. In spite of decreased Mapk3 mRNA, no modifications in the expression of ERK1 (Genotype effect: $F_{(1, 31)}$ = 3.13, *N.S.*; Treatment effect: $F_{(3, 31)}$ = 2.15, *N.S.*; Interaction: $F_{(3, 31)}$ = 1.26, *N.S.*) were seen in treated AβPP/PS1 mice (Figure 5A). However, natural cannabinoids induced a significant modulation of ERK1, but not ERK2, phosphorylation (Genotype effect: $F_{(1, 31)}$ = 0.93, *N.S.*; Treatment effect: $F_{(3, 31)}$ = 5.18, p < 0.01; Interaction: $F_{(3, 31)}$ = 3.73, p < 0.05). Thus, CBD increased the levels of phospho-ERK1 in wild-type animals when compared to the vehicle (p < 0.05) or THC+CBD (p < 0.01) groups. In contrast, THC and THC+CBD induced a tendency to reduce the phosphorylation of ERK1 in AβPP/PS1 mice, which was apparently enhanced in vehicle-treated transgenic animals (Figure 5A). Those results indicate that cannabinoid compounds could differentially regulate ERK1 signaling.

Natural cannabinoids modulated the levels of Txn2 in treated mice (Genotype effect: $F_{(1, 31)}$ = 0.71, *N.S.*; Treatment effect: $F_{(3, 31)}$ = 5.56, p < 0.01; Interaction: $F_{(3, 31)}$ = 9.22, p < 0.001). AβPP/PS1 mice exhibited decreased Txn2 protein levels after treatment with vehicle (p < 0.05) and THC (p < 0.05), which was also apparent but not significant after CBD exposure, when compared to wild-type littermates (Figure 5B). This deficiency in

Txn2 levels could account to impaired capability to cope with oxidative components in AβPP/PS1 mice. Interestingly, the combination of THC+CBD induced a strong increase in the Txn2 protein levels ($p < 0.01$ with respect to vehicle or CBD; $p < 0.001$ with respect to THC), which completely reversed this Txn2 deficiency observed in AβPP/PS1 mice (Figure 5B).

Regarding the signaling protein Wnt16, a significant effect of treatment was also observed (Genotype effect: $F_{(1, 31)} = 2.59$, *N.S.*; Treatment effect: $F_{(3, 31)} = 5.64$, $p < 0.01$; Interaction: $F_{(3, 31)} = 1.67$, *N.S.*). Both THC and the combination of THC+CBD increased the levels in AβPP/PS1 mice when compared to vehicle-treated animals ($p < 0.05$). THC-treated AβPP/PS1 mice exhibited significantly higher Wnt16 protein levels than corresponding wild-type controls ($p < 0.01$) (Figure 5C).

Discussion

According to the protective hypothesis of cannabinoid compounds in neurodegenerative diseases, the present findings show that treatment with natural cannabinoids at non-psychoactive doses reduces cognitive impairment and several pathological processes occurring in AβPP/PS1, a model of AD, when chronically administered at the early symptomatic phase. Thus, THC and CBD, as well as the combination of both natural cannabinoids, reduces memory impairment exhibited by AβPP/PS1 mice in the two-object recognition test, but only the combination of THC+CBD was able to prevent learning deficiency of transgenic mice in the active avoidance test, considered a complex cognitive task. As THC and CBD are supposed to produce their effects by acting on different signaling pathways [23], the present results with combined THC and CBD can be interpreted as a summative effect or as an interaction of the two compounds resulting in the potentiation of each cannabinoid, as previously suggested [24, 25]. The present findings are in agreement with a recent report conducted in parallel demonstrating positive behavioral effects of THC+CBD in a murine model of tauopathy [10]. Importantly, the cannabinoid doses employed in this study are devoid of psychoactivity [26] and their HED corresponds to a single Sativex® administration, what means that the potential translation of our results to human beings might result in a safe and well-tolerated approach taking into consideration that multiple sclerosis patients receiving up to 12 Sativex® administrations per day reported a relatively low side-effect profile [27].

A collateral observation deserves attention. In contrast to AβPP/PS1 mice, memory impairment occurs in wild-type mice chronically exposed to the THC-enriched extract at doses that are known not to produce acute amnesia-like effects in mice [26]. This observation warns about the chronic effects of THC in healthy individuals and is in

accordance with several human studies revealing that long-term use of cannabis can be associated with disruption of short-term memory, working memory, and attention skills [28, 29]. It is known that certain cannabinoids, such as THC, affect cognitive function modulating signaling pathways critically implicated in learning and memory [30]. The molecular reorganization of endogenous cannabinoid system in AD [31] and the altered neuronal signaling occurring during the neurodegenerative processes may account for the discrepancy between the effects of THC in wild-type and AD-like transgenic mice. However, wild-type mice chronically receiving THC+CBD do not exhibit memory impairment. This observation supports previous work showing that CBD is able to antagonize THC-induced deficits in memory tasks [32], and highlights the relevance of combining the two natural cannabinoids, THC and CBD, to mitigate the negative consequences of THC administration.

A remarkable finding of this study is the altered Aβ processing induced by the THC+CBD combination in AβPP/PS1 mice. Even though THC, CBD, and the combination of both did not significantly modify cortical or hippocampal Aβ burden in AβPP/PS1 mice in spite of a tendency to decrease in the animals treated with THC+CBD, the combination of both compounds reduced soluble $A\beta_{42}$, but not $A\beta_{40}$ protein levels, thus showing a protective effect by reducing the quantity of the most toxic soluble Aβ form in AβPP/PS1 animals [33]. We have also observed a change in amyloid plaques composition since an increase in the $A\beta_{42}/A\beta_{40}$ ratio in each plaque was observed in THC+CBD-treated AβPP/PS1 mice, suggesting a cannabinoid-induced facilitation of the $A\beta_{42}$ deposition that could account at least in part for the specific reduction of soluble $A\beta_{42}$ observed and likely to decrease its toxicity. The recently described $A\beta_{42}$ clearance facilitation across the blood brain barrier by cannabinoids [8,

34], might also contribute to the THC-CBD-induced reduction of the Aβ toxicity in our AD model.

AD progression involves aberrant glial activation and neuroinflammation that contribute to neuronal dysfunction, which in turn drives a vicious cycle of further glial activation and neuronal damage [35]. Several studies have shown anti-inflammatory effects of natural and synthetic CB_1 or CB_2 agonists, as well as CBD, in multiple *in vitro* and *in vivo* AD models [6, 7, 8, 14, 36, 37, 38]. The present observations confirm previous findings by demonstrating a reduction of the astrogliosis associated with Aβ deposition in AβPP/PS1 mice treated with THC, CBD, or the combination of both. In addition, THC+CBD significantly reduced microgliosis and the expression of several cytokines and related molecules in AβPP/PS1 mice. Most importantly, the combination of THC+CBD resulted more effective than either THC or CBD alone.

The ubiquitous distribution of endocannabinoid system and its polyvalent functionality suggest that the positive cognitive effects observed in AβPP/PS1 after chronic treatment with natural cannabinoids might be due to multiple mechanisms run in parallel, beyond to the already known anti-inflammatory properties or the role in reducing Aβ toxicity. A useful tool to identify novel mechanisms that may contribute to a certain effect is the microarrays technology. This technique involves large-scale monitoring of relative differences in RNA abundance between samples. Thus, we identified additional mechanisms contributing to the natural cannabinoid effects in AβPP/PS1 mice by RNA microarrays. The functional analysis of the results pointed to molecular degradation, immunomodulation, mitochondrial function, and Mapk3 and Wnt16 signaling pathways, among others, as relevant pathways targeted by cannabinoids. First, we focused on validating the cannabinoid effects on the Mapk3 signaling. Previous *in vitro* studies have shown that the stimulation of endogenous

cannabinoid system decreases ERK1/2 pro-inflammatory signaling in response to Aβ, resulting in reduced toxicity [12, 39]. Although the total amount of ERK1, the protein coded by Mapk3, is not significantly modulated by cannabinoids in the present model, THC and THC+CBD decrease ERK1 phosphorylation. We also observed an increase in ERK1/2 phosphorylation in wild-type animals receiving CBD, which is contrast to a previous study showing reduced phospho-ERK1/2 in the cortex of rats chronically exposed to CBD [40]. These discrepancies could be due to different experimental conditions. Together, these observations point to the need for further studies geared to elucidating the ERK response in wild and AβPP/PS1 mice treated with cannabinoids.

Another important contribution of the present study is the induction of Txn2 protein levels by the THC+CBD combination, in contrast to the reduced Txn2 mRNA expression observed in the microarray study as well as by quantitative PCR. The divergence between the mRNA and protein levels could account for compensatory mechanisms directed to regulate Txn2 functionality. THC+CBD completely reversed Txn2 deficiency in AβPP/PS1 mice, which also occurs in AD patients [41]. This nuclear gene encodes a mitochondrial member of the thioredoxin family, a group of small multifunctional redox-active proteins [42]. The encoded protein is a key component of the mitochondrial antioxidant system which is responsible for the clearance of reactive intermediates and repairs proteins with oxidative damage and may play important roles in the regulation of the mitochondrial membrane potential and in protection against oxidant-induced apoptosis [43, 44]. Therefore, it can be assumed that increased Txn2 levels provide protection against oxidative damage in our model.

Finally, little is known about the role of Wnt16 signaling in cells and to our knowledge there is no specific information about Wnt16 function in brain. The Wnt gene family consists of structurally related genes which encode secreted signaling proteins. These

proteins have been implicated in oncogenesis and in several developmental processes, including regulation of cell fate and patterning during embryogenesis, as well as in axon guidance during development and in response to traumatic injury in adult central nervous system [45]. Moreover, activation of the Wnt signaling pathway prevents Aβ-induced neurotoxicity *in vitro*, probably through the modulation of the GSK3β/β-catenin pathway [46]. Wnt16 gene is a member of the Wnt gene family. It contains two transcript variants diverging at the 5' termini. These two variants are proposed to be the products of separate promoters and not to be splice variants from a single promoter. They are differentially expressed in normal tissues, one of which (variant 2) is expressed at significant levels only in the pancreas, whereas another one (variant 1) is expressed more ubiquitously with highest levels in adult kidney, placenta, brain, heart, and spleen [47]. Thus, it is tempting to speculate that increased cannabinoid-induced Wnt16 expression may reduce Aβ neurotoxicity and contribute to maintain axon integrity *in vivo*. Nevertheless, additional experiments are required to validate this hypothesis.

In summary, here we provide evidence of the therapeutic effects of the THC+CBD combination, over THC or CBD alone, by acting at different levels modifying Aβ metabolism, reducing soluble $A\beta_{42}$ levels, astrogliosis, microglia, and several molecules of neuroinflammation. Speculatively, it is conceivable that the effects of THC+CBD combination are also due to the increase protein expression of thioredoxin 2 and Wnt16. Nevertheless, additional experiments are required to validate this hypothesis. This is accompanied by a reduction of memory deficits and increased learning capacity in AβPP/PS1 transgenic mice used as a model of AD. The present findings give insights for a further clinical trial to test the effectiveness of THC+CBD in AD patients.

Acknowledgements

We thank T. Yohannan for editorial help and GW Pharmaceuticals Ltd for the supply of the botanical extracts. This study was supported by grants from the Agrupació Mútua Foundation (XVII Award in the Elderly Field, to IF), Mutua Madrileña Foundation (IF), and BESAD-P project, CIBERNED, Instituto Carlos III (IF).

Statement of Interest

None.

References

[1] Ferrer I (2012) Defining Alzheimer as a common age-related neurodegenerative process not inevitably leading to dementia. *Prog Neurobiol* **97**, 38-51.

[2] Selkoe DJ (2012) Preventing Alzheimer's disease. *Science* **337**, 1488-1492.

[3] Campbell VA, Gowran A (2007) Alzheimer's disease; taking the edge off with cannabinoids? *Br J Pharmacol* **152**, 655-662.

[4] Koppel J, Davies P (2008) Targeting the endocannabinoid system in Alzheimer's disease. *J Alzheimers Dis* **15**, 495-504.

[5] Aso E, Ferrer I (2014) Cannabinoids for treatment of Alzheimer's disease: moving toward the clinic. *Front Pharmacol* **5**, 37.

[6] Aso E, Palomer E, Juvés S, Maldonado R, Muñoz FJ, Ferrer I (2012) CB_1 agonist ACEA protects neurons and reduces the cognitive impairment of AβPP/PS1 mice. *J Alzheimers Dis* **30**, 439-459.

[7] Aso E, Juvés S, Maldonado R, Ferrer I (2013) CB_2 cannabinoid receptor agonist ameliorates Alzheimer-like phenotype in AβPP/PS1 mice. *J Alzheimers Dis*. **35**, 847-858.

[8] Martín-Moreno AM, Brera B, Spuch C, Carro E, García-García L, Delgado M, Pozo MA, Innamorato NG, Cuadrado A, de Ceballos ML (2012) Prolonged oral cannabinoid administration prevents neuroinflammation, lowers β-amyloid levels and improves cognitive performance in Tg APP 2576 mice. *J Neuroinflammation* **9**, 8.

[9] Wu J, Bie B, Yang H, Xu JJ, Brown DL, Naguib M (2013) Activation of the CB(2) receptor system reverses amyloid-induced memory deficiency. *Neurobiol Aging* **34**, 791-804.

[10] Casarejos MJ, Perucho J, Gómez A, Muñoz MP, Fernández-Estévez M, Sagredo O, Fernández Ruiz J, Guzmán M, de Yébenes JG, Mena MA (2013) Natural cannabinoids

improve dopamine neurotransmission and tau and amyloid pathology in a mouse model of tauopathy. *J Alzheimers Dis* **35**, 525-539.

[11] Noonan J, Tanveer R, Klompas A, Gowran A, McKiernan J, Campbell VA (2010) Endocannabinoids prevent beta-amyloid-mediated lysosomal destabilization in cultured neurons. *J Biol Chem* **285**, 38543-38554.

[12] Chen X, Zhang J, Chen C (2011) Endocannabinoid 2-arachidonoylglycerol protects neurons against β-amyloid insults. *Neuroscience* **178**, 159-168.

[13] Tolón RM, Núñez E, Pazos MR, Benito C, Castillo AI, Martínez-Orgado JA, Romero J (2009) The activation of cannabinoid CB_2 receptors stimulates in situ and in vitro beta-amyloid removal by human macrophages. *Brain Res* **1283**, 148-154.

[14] Martín-Moreno AM, Reigada D, Ramírez BG, Mechoulam R, Innamorato N, Cuadrado A, de Ceballos ML (2011) Cannabidiol and other cannabinoids reduce microglial activation in vitro and in vivo: relevance to Alzheimer's disease. *Mol Pharmacol* **79**, 964-973.

[15] Esposito G, De Filippis D, Carnuccio R, Izzo AA, Iuvone T (2006a) The marijuana component cannabidiol inhibits beta-amyloid-induced tau protein hyperphosphorylation through Wnt/beta-catenin pathway rescue in PC12 cells. *J Mol Med* **84**, 253-258.

[16] Esposito G, De Filippis D, Steardo L, Scuderi C, Savani C, Cuomo V, Iuvone T (2006b) CB_1 receptor selective activation inhibits beta-amyloid-induced iNOS protein expression in C6 cells and subsequently blunts tau protein hyperphosphorylation in co-cultured neurons. *Neurosci Lett* **404**, 342-346.

[17] Barnes MP (2006) Sativex: clinical efficacy and tolerability in the treatment of symptoms of multiple sclerosis and neuropathic pain. *Expert Opin Pharmacother* **7**, 607-615.

[18] Pazos MR, Sagredo O, Fernández-Ruiz J (2008) The endocannabinoid system in Huntington's disease. *Curr Pharm Des* **14**, 2317-2325.

[19] Borchelt DR, Ratovitski T, van Lare J, Lee MK, Gonzales V, Jenkins NA, Copeland NG, Price DL, Sisodia SS (1997) Accelerated amyloid deposition in the brains of transgenic mice coexpressing mutant presenilin 1 and amyloid precursor proteins. *Neuron* **19**, 939-945.

[20] Reagan-Shaw S, Nihal M, Ahmad N (2008) Dose translation from animal to human studies revisited. *FASEB J*, **22**, 659-661.

[21] Aso E, Lomoio S, López-González I, Joda L, Carmona M, Fernández-Yagüe N, Moreno J, Juvés S, Pujol A, Pamplona R, Portero-Otín M, Martín V, Díaz M, Ferrer I (2012) Amyloid generation and dysfunctional immunoproteasome activation with disease progression in animal model of familial Alzheimer's disease. *Brain Pathol* **22**, 636-653.

[22] Durrenberger PF, Fernando FS, Magliozzi R, Kashefi SN, Bonnert TP, Ferrer I, Seilhean D, Nait-Oumesmar B, Schmitt A, Gebicke-Haerter PJ, Falkai P, Grünblatt E, Palkovits M, Parchi P, Capellari S, Arzberger T, Kretzschmar H, Roncaroli F, Dexter DT, Reynolds R (2012) Selection of novel reference genes for use in the human central nervous system: a BrainNet Europe Study. *Acta Neuropathol* **124**, 893-903.

[23] Huestis MA (2005) Pharmacokinetics and metabolism of the plant cannabinoids, delta9-tetrahydrocannabinol, cannabidiol and cannabinol. *Handb Exp Pharmacol* **168**, 657-690.

[24] Varvel SA, Wiley JL, Yang R, Bridgen DT, Long K, Lichtman AH, Martin BR (2006) Interactions between THC and cannabidiol in mouse models of cannabinoid activity. *Psychopharmacology (Berl)* **186**, 226-234.

[25] Klein C, Karanges E, Spiro A, Wong A, Spencer J, Huynh T, Gunasekaran N, Karl T, Long LE, Huang XF, Liu K, Arnold JC, McGregor IS (2011) Cannabidiol potentiates Δ9-tetrahydrocannabinol (THC) behavioural effects and alters THC pharmacokinetics during acute and chronic treatment in adolescent rats. *Psychopharmacology (Berl)* **218**, 443-457.

[26] Puighermanal E, Marsicano G, Busquets-Garcia A, Lutz B, Maldonado R, Ozaita A (2009) Cannabinoid modulation of hippocampal long-term memory is mediated by mTOR signaling. *Nat Neurosci* **12**, 1152-1158.

[27] Wade DT, Collin C, Stott C, Duncombe P (2010) Meta-analysis of the efficacy and safety of Sativex (nabiximols), on spasticity in people with multiple sclerosis. *Mult Scler* **16**, 707-714

[28] Fletcher JM, Page JB, Francis DJ, Copeland K, Naus MJ, Davis CM, Morris R, Krauskopf D, Satz P (1996) Cognitive correlates of long-term cannabis use in Costa Rican men. *Arch Gen Psychiatry* **53**, 1051-1057.

[29] Iversen L (2003) Cannabis and the brain. *Brain* **126**, 1252-1270.

[30] Puighermanal E, Busquets-Garcia A, Maldonado R, Ozaita A (2012) Cellular and intracellular mechanisms involved in the cognitive impairment of cannabinoids. *Philos Trans R Soc Lond B Biol Sci* **367**, 3254-3263.

[31] Mulder J, Zilberter M, Pasquare SJ, Alpar A, Schulte G, Ferreira SG, Kofalvi A, Martín-Moreno AM, Keimpema E, Tanila H,Watanabe M, Mackie K, Hortobagyi T, de Ceballos ML, Harkany T (2011) Molecular reorganization of endocannabinoide signalling in Alzheimer's disease. *Brain* **134**, 1041-1060.

[32] Fadda P, Robinson L, Fratta W, Pertwee RG, Riedel G (2004) Differential effects of THC- or CBD-rich cannabis extracts on working memory in rats. *Neuropharmacology* **47**, 1170-1179.

[33] Mucke L, Selkoe DJ. (2012) Neurotoxicity of amyloid β-protein: synaptic and network dysfunction. *Cold Spring Harb Perspect Med* **2**, a006338.

[34] Bachmeier C, Beaulieu-Abdelahad D, Mullan M, Paris D (2013) Role of the cannabinoid system in the transit of beta-amyloid across the blood-brain barrier. *Mol Cell Neurosci* **56**, 255-262.

[35] Mrak RE, Griffin WS (2005) Glia and their cytokines in progression of neurodegeneration. *Neurobiol Aging* **26**, 349-354.

[36] van der Stelt M, Mazzola C, Esposito G, Matias I, Petrosino S, De Filippis D, Micale V, Steardo L, Drago F, Iuvone T, Di Marzo V (2006) Endocannabinoids and beta-amyloid-induced neurotoxicity *in vivo*: effect of pharmacological elevation of endocannabinoid levels. *Cell Mol Life Sci* **63**, 1410-1424.

[37] Esposito G, Iuvone T, Savani C, Scuderi C, De Filippis D, Papa M, Di Marzo V, Steardo L (2007) Opposing control of cannabinoid receptor stimulation on amyloid-beta-induced reactive gliosis: *in vitro* and *in vivo* evidence. *J Pharmacol Exp Ther* **322**, 1144-1152.

[38] Ramírez BG, Blázquez C, Gómez del Pulgar T, Guzmán M, de Ceballos ML (2005) Prevention of Alzheimer's disease pathology by cannabinoids: neuroprotection mediated by blockade of microglial activation. *J Neurosci* **25**, 1904-1913.

[39] Benito C, Tolón RM, Castillo AI, Ruiz-Valdepeñas L, Martínez-Orgado JA, Fernández-Sánchez FJ, Vázquez C, Cravatt BF, Romero J (2012) β-Amyloid exacerbates inflammation in astrocytes lacking fatty acid amide hydrolase through a mechanism involving PPAR-α, PPAR-γ and TRPV1, but not CB_1 or CB_2 receptors. *Br J Pharmacol* **166**, 1474-1489.

[40] ElBatsh MM, Assareh N, Marsden CA, Kendall DA (2012) Anxiogenic-like effects of chronic cannabidiol administration in rats. *Psychopharmacology (Berl)* **221**, 239-247.

[41] Lovell MA, Xie C, Gabbita SP, Markesbery WR (2000) Decreased thioredoxin and increased thioredoxin reductase levels in Alzheimer's disease brain. *Free Radic Biol Med* **28**, 418-427.

[42] Arnér ES (2009) Focus on mammalian thioredoxin reductases-important selenoproteins with versatile functions. *Biochim Biophys Acta* **1790**, 495-526.

[43] Chen Y, Yu M, Jones DP, Greenamyre JT, Cai J (2006) Protection against oxidant-induced apoptosis by mitochondrial thioredoxin in SH-SY5Y neuroblastoma cells. *Toxicol Appl Pharmacol* **216**, 256-262.

[44] Damdimopoulos AE, Miranda-Vizuete A, Pelto-Huikko M, Gustafsson JA, Spyrou G (2002) Human mitochondrial thioredoxin. Involvement in mitochondrial membrane potential and cell death. *J Biol Chem* 277, 33249-33257.

[45] Onishi K, Hollis E, Zou Y (2014) Axon guidance and injury-lessons from Wnts and Wnt signaling. *Curr Opin Neurobiol* **27C**, 232-240.

[46] Inestrosa NC, Montecinos-Oliva C, Fuenzalida M (2012) Wnt signaling: role in Alzheimer disease and schizophrenia. *J Neuroimmune Pharmacol* **7**, 788-807.

[47] Fear MW, Kelsell DP, Spurr NK, Barnes MR (2000) Wnt-16a, a novel Wnt-16 isoform, which shows differential expression in adult human tissues. *Biochem Biophys Res Commun* **278**, 814-820.

Table 1. mRNA expression levels of several cytokine-related genes involved in the inflammatory response in AβPP/PS1 mice.

	Cytokine-related genes	AβPP/PS1			
		Vehicle	**THC**	**CBD**	**THC+CBD**
Anti-inflammatory cytokines	Il10ra	1.02 ± 0.09	0.90 ± 0.05	0.92 ± 0.07	0.88 ± 0.06
	Il10rb	1.01 ± 0.07	1.08 ± 0.04	0.96 ± 0.08	0.78 ± 0.03 *§
	Tgfb1	1.03 ± 0.12	0.86 ± 0.05	0.84 ± 0.08	0.71 ± 0.07 *
Cell Surface Adhesion	Itgb2	1.01 ± 0.07	0.95 ± 0.05	1.04 ± 0.15	0.75 ± 0.08 *
Chemokines	Ccl3	1.04 ± 0.12	1.21 ± 0.14	1.19 ± 0.10	0.82 ± 0.16
	Ccl4	1.03 ± 0.10	1.16 ± 0.10	1.39 ± 0.10 *	0.97 ± 0.17
	Ccl6	1.04 ± 0.12	1.24 ± 0.09	1.19 ± 0.12	0.99 ± 0.09
	CxCl10	1.22 ± 0.35	1.21 ± 0.21	1.04 ± 0.19	0.95 ± 0.18
Complement system	C1ql1	1.01 ± 0.05	1.15 ± 0.05	1.04 ± 0.03	1.11 ± 0.13
	C1qtnf7	1.08 ± 0.19	0.95 ± 0.08	0.99 ± 0.03	0.75 ± 0.08 &
	C3ar1	1.00 ± 0.04	0.99 ± 0.04	1.03 ± 0.07	0.91 ± 0.06
	C4b	1.02 ± 0.09	0.89 ± 0.03	1.07 ± 0.12	0.87 ± 0.12
Colony stimulating factor receptors	Csf1r	1.01 ± 0.05	1.01 ± 0.03	0.96 ± 0.05	0.90 ± 0.05
	Csf3r	1.02 ± 0.08	1.02 ± 0.10	0.86 ± 0.05	0.71 ± 0.07 *§
Fc receptors	Fcgr1	1.02 ± 0.09	1.08 ± 0.06	1.00 ± 0.06	0.85 ± 0.08 §
	Fcgr2b	1.01 ± 0.07	1.11 ± 0.07	1.08 ± 0.09	0.87 ± 0.05 §
Pro-inflammatory cytokines	Il6st	1.01 ± 0.06	0.95 ± 0.07	0.98 ± 0.07	0.77 ± 0.07 *
	Tnfrsf1a	1.02 ± 0.08	1.15 ± 0.08	1.15 ± 0.05	1.12 ± 0.09
Regulator of myeloid cells	Inpp5d	1.01 ± 0.05	0.92 ± 0.08	0.82 ± 0.10	0.60 ± 0.09 *§
Toll-like receptors	Tlr4	1.02 ± 0.09	0.90 ± 0.11	0.80 ± 0.08	0.68 ± 0.05 *
	Tlr7	1.06 ± 0.15	1.01 ± 0.11	0.96 ± 0.16	0.63 ± 0.06 *§

Values are calculated with the ΔΔCt method, using the mean of three housekeeping genes (Aars, Hprt, Xpnpep1) and vehicle-treated AβPP/PS1 as references. * $p < 0.05$ *vs* Vehicle; § $p < 0.05$ *vs* THC; & $p < 0.05$ *vs* CBD.

Supplementary Table S1. Total exploration time in the two-object recognition test.

Genotype	Treatment	Total Exploration Time (sec)	
		Memory Acquisition	Memory Test
WT	**Veh**	50.11 ± 16.10	48.59 ± 15.03
	THC	31.86 ± 5.00	21.72 ± 2.96
	CBD	36.55 ± 8.27	28.35 ± 6.52
	THC+CBD	52.65 ± 6.60	35.25 ± 8.19
AβPP/PS1	**Veh**	36.29 ± 6.38	20.64 ± 4.30
	THC	52.22 ± 5.47	34.07 ± 6.19
	CBD	38.02 ± 7.70	28.94 ± 8.53
	THC+CBD	48.56 ± 9.63	23.77 ± 6.24

Data are expressed as mean ± SEM. No significant difference was observed with two-way ANOVA in the memory acquisition or the memory test total exploration time.

Supplementary Table S2. Statistical analysis of the natural cannabinoids effects on the learning capacity of AβPP/PS1 mice in the active avoidance test.

Conditioned changes					
Two-way ANOVA	VEH	THC	CBD	THC+CBD	
Factors					
Day (repeated)	$F_{(4,52)} = 18.62$, $p<0.001$	$F_{(4,72)} = 30.92$, $p<0.001$	$F_{(4,48)} = 20.12$, $p<0.001$	$F_{(4,52)} = 24.19$, $p<0.001$	
Genotype	$F_{(1,13)} = 9.03$, $p<0.01$	*N.S.*	$F_{(1,12)} = 9.96$, $p<0.01$	*N.S.*	
Interaction	$F_{(4,52)} = 5.45$, $p<0.001$	$F_{(4,72)} = 2.79$, $p<0.05$	$F_{(4,48)} = 3.49$, $p<0.05$	*N.S.*	
Genotype comparisons	Day1	Day2	Day3	Day4	Day5
VEH	*N.S.*	*N.S.*	$p<0.05$	$p<0.01$	$p<0.001$
THC	*N.S.*	*N.S.*	*N.S.*	*N.S.*	$p<0.05$
CBD	$p<0.05$	*N.S.*	$p<0.05$	$p<0.01$	$p<0.01$
THC+CBD	*N.S.*	*N.S.*	*N.S.*	*N.S.*	*N.S.*
Area under the curve (AUC)					
Two-way ANOVA					
Factors		VEH	THC	CBD	THC+CBD
Genotype	$F_{(1,57)} = 14.77$, $p<0.001$	$p<0.01$	*N.S.*	$p<0.05$	*N.S.*
Treatment	*N.S.*				
Interaction	*N.S.*				

Two-way ANOVA with day (repeated measures) and genotype as between-subjects factor was applied for the analysis of conditioned changes (learning). For the AUC analysis, two-way ANOVA with genotype and treatment as between-subjects factors was applied. *N.S.*, not significant difference. See Materials and methods for details.

Supplementary Table S3. Functional analysis for regulated genes in treated AβPP/PS1.

Comparison	KEGG ID	*P* value	Term	Regulated Gene Names
THC *vs* VEH				
	4012	0.0077	ErbB signaling pathway	Btc, Gab1, Nrg1, ***Mapk3***, Nrg4
	4140	0.0102	Regulation of autophagy	Ulk1, Atg12, Gabarap
	3018	0.0171	RNA degradation	Eno3, Parn, Btg2, Lsm3
	5012	0.0320	Parkinson's disease	***Cox7c***, Ndufa9, ***Ubb***, Vdac1, Cox6b2
	4150	0.0354	mTOR signaling pathway	Pdpk1, ***Mapk3***, Ulk1
	4621	0.0489	NOD-like receptor signaling pathway	***Mapk3***, Ccl2, Traf6
CBD *vs* VEH				
	4916	0.0050	Melanogenesis	***Adcy3***, Kit, Plcb4, Mapk2k2, Fzd9, **Wnt16**
	3013	0.0289	RNA transport	Gemin2, Eif3f, Srrm1, Pop1, Gemin8, Nup35
	3050	0.0316	Proteasome	Psmb1, ***Psmb2***, Psmd4
	5200	0.0318	Pathways in cancer	Cbl, Cebpa, Fgf2, Fgf4, Kit, Map2k2, Traf1, Fzd9, Ralbp1, ***Wnt16***
THC+CBD *vs* VEH				
	5140	0.0041	Leishmaniasis	Cr1, Fcgr3a, Hla-Dpb1, Irak1, ***Mapk3***
	4740	0.0049	Olfactory transduction	***Adcy3***, Or1e1, Or2ae1, Or8i2, Or10a7, Or2t4, Or6n1, Or13c8, Or10a5, Or8j1, Or5ar1, Or51i2, Or8h3
	4145	0.0074	Phagosome	Fcgr2b, Fcgr3a, Hla-Dpb1, ***Nos1***, Cd209, Tuba1c, Tubb8
	330	0.0084	Arginine and proline metabolism	Aldh9a1, Arg1, Gamt, ***Nos1***
	5221	0.0108	Acute myeloid leukemia	Cebpa, Kit, ***Mapk3***, Pim2
	4612	0.0259	Antigen processing and presentation	Hla-Dpb1, Klrc2, Tapbp, Rfxank
	4380	0.0428	Osteoclast differentiation	Fcgr2b, Fcgr3a, Jund, ***Mapk3***, Socs3
	5322	0.0440	Systemic lupus erythematosus	Fcgr2b, Fcgr3a, Hist1h2bb, Hla-Dpb1, H3f3c
	5150	0.0444	Staphylococcus aureus infection	Fcgr2b, Fcgr3a, Hla-Dpb1
	3060	0.0474	Protein export	Srp14, Spcs1
	4540	0.0480	Gap junction	***Adcy3, Mapk3***, Tuba1c, Tubb8

Genes names highlighted in bold and italics were chosen for validation by RT-PCR.

Figure 1: (A) Memory performance of animals treated during the early symptomatic stage (6 months). AβPP/PS1 mice chronically treated with vehicle exhibit a significant reduction in the recognition index when compared to corresponding wild-type littermates. However, chronic THC (0.75 mg/kg, i.p.), CBD (0.75 mg/kg, i.p.) botanical extracts, and THC+CBD (0.75 mg/kg each, i.p.) administration induce memory improvement in AβPP/PS1 when compared to wild-type animals. Interestingly, chronic THC induces a significant reduction in the memory performance of wild-type animals. (B-F) The number of conditioned changes in the active avoidance test was recorded during 5 consecutive days in order to evaluate the learning performance of mice. (B) Statistical analysis from the Area Under the Curve (AUC) reveals a global reduction in the learning performance of vehicle- and CBD-treated but not in THC- or THC+CBD-treated AβPP/PS1 mice when compared to wild littermates. The comparison of the conditioned changes achieved by mice every training day reveals a significant reduction in AβPP/PS1 mice treated with vehicle from day 3 to day 5 (C), in THC-treated on day 5 (D) and in CBD-treated mice from day 3 to day 5 (E) when compared with wild-type animals. In contrast, AβPP/PS1 mice chronically treated with the combination of THC+CBD do not evidence such learning impairment at any day, thus demonstrating a positive effect (F). No significant treatment effect is observed respect vehicle group either in wild-type (light gray dashed line) or AβPP/PS1 mice (dark gray dashed line). Data are expressed as the mean values ± SEM. ★ $p < 0.05$, ★★ $p < 0.01$ ★★★ $p < 0.001$ genotype effect; ☆ $p < 0.05$, ☆☆ $p < 0.01$, ☆☆☆ $p < 0.001$ compared to vehicle. § $p < 0.05$ compared to THC group.

Figure 2: (A) Scheme showing the cortical brain areas (dashed squares) analyzed for Aβ burden quantification in each animal. Neither total Aβ burden (B) nor $Aβ_{42}$ or $Aβ_{40}$ burden (C) are significantly modified in AβPP/PS1 mice cortex by chronic treatment

with THC, CBD, or the combination of the two, in spite of the tendency toward decrease in THC+CBD-treated animals. (D) Soluble $A\beta_{40}$ and $A\beta_{42}$ levels in cortical homogenates from AβPP/PS1 mice chronically treated with THC, CBD, and THC+CBD during the early symptomatic phase. The THC+CBD combination significantly reduces protein levels of soluble $A\beta_{42}$ when compared to vehicle-treated controls, revealing the protective effect of the combination of the natural cannabinoids. (E) Reduction in the $A\beta_{42}$ soluble contents can be related, in part, to a change in the composition of plaques since THC+CBD-treated AβPP/PS1 mice present increased $A\beta_{42}$ respect $A\beta_{40}$ deposition in each plaque when compared to vehicle-treated animals. (F) Representative images of the $A\beta_{42}$ (right) and $A\beta_{40}$ (left) specific immunoreactivity in consecutive cortical sections of AβPP/PS1 mice treated during the early symptomatic phase. Scale bar represents 100 μm. Counts are expressed as the mean values ± SEM. ★ $p < 0.05$, ★★ $p < 0.01$ compared to vehicle. § $p < 0.05$ compared to THC group. & $p < 0.05$ compared to CBD group.

Figure 3: (A) Representative images of double GFAP (red, upper panels) or IBA1 (red, lower panels) and Aβ (green) immunoreactivity in cortical sections of AβPP/PS1 mice chronically treated during the early symptomatic phase with natural cannabinoids. Scale bar represents 25 μm. (B) Quantification of the GFAP staining around the Aβ plaques reveals a significant reduction of the astroglial response in AβPP/PS1 mice chronically treated with THC, CBD, or the combination of the two. (C) Quantification of the IBA1 staining around the Aβ plaques reveals a significant reduction in microglial response only in AβPP/PS1 mice chronically treated with the combination of THC+CBD. Data are expressed as the mean values ± SEM. ★ $p < 0.05$, ★★ $p < 0.01$ ★★★ $p < 0.001$compared to vehicle.

Figure 4: (A) Heat map generated from RNA microarray data reflecting the differential gene expression profile induced by cannabinoid compounds. Blue: decreased expression. Red: increased expression. Headings: Vehicle (yellow), THC (blue), CBD (green), THC+CBD (red). (B) Venn's diagram showing the number of genes significantly regulated by natural cannabinoids. (C) Real-time PCR validated the results obtained with microarray techniques in at least 4 out of 8 candidate genes, confirming decreased expression of Mapk3, Psmb2, Txn2, and Wnt16 genes in THC+CBD-treated AβPP/PS1 mice. Data are expressed as the mean values ± SEM. ★ $p < 0.05$ compared to vehicle. & $p < 0.05$, && $p < 0.01$ compared to CBD.

Figure 5: Western blot quantification of proteins codified by genes differentially expressed in treated mice: ERK1 (Mapk3), thioredoxin 2 (Txn2), and wingless-related integration site (Wnt16). (A) No significant change in the total amount of ERK1 is observed in any treatment group, in spite of the tendency toward increased total ERK1 in THC+CBD-treated AβPP/PS1 mice. CBD significantly increases the levels of phosphorylated ERK1 in wild-type animals. In contrast, THC and THC+CBD slightly decrease ERK1 phosphorylation without statistical significance. (B) THC+CBD completely reverses the Txn2 deficiency exhibited by vehicle- and THC-treated AβPP/PS1 mice. (C) THC and THC+CBD increase the levels of Wnt16 protein in cortical homogenates of AβPP/PS1 treated mice. In the upper part of each panel are representative immunoblots for ERK1/2, Txn2, and Wnt16, and corresponding tubulin loading control. Densitometric quantifications are expressed as the mean values ± SEM. ★ $p < 0.05$, ★★ $p < 0.01$ genotype effect. ☆ $p < 0.05$, ☆☆ $p < 0.01$, compared to vehicle. §§§ $p < 0.001$ compared to THC. && $p < 0.01$ compared to CBD.

Figure 1

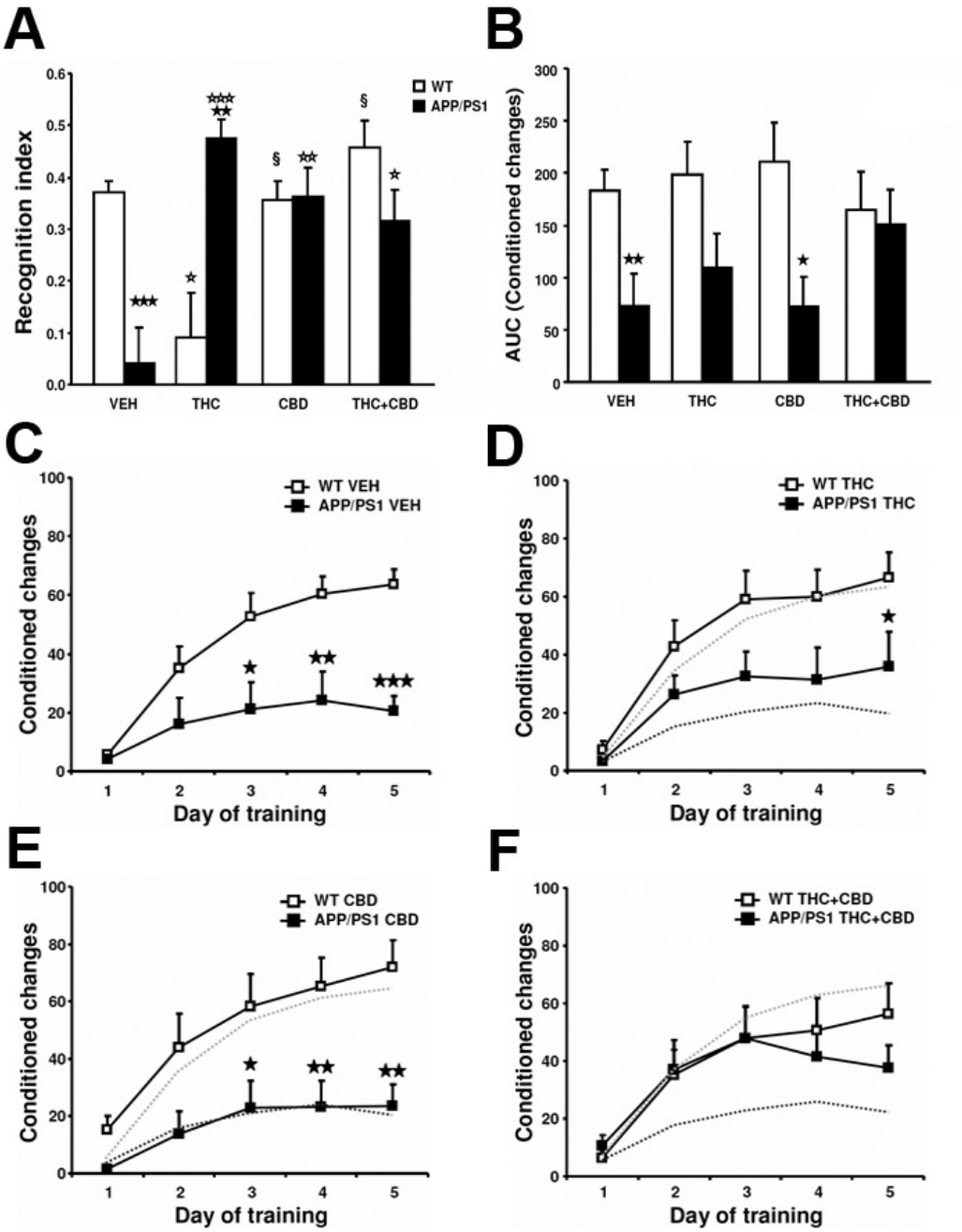
A
B
C
D
E
F
Recognition index
WT
APP/PS1
VEH
THC
CBD
THC+CBD
AUC (Conditioned changes)
Conditioned changes
Day of training
WT VEH
APP/PS1 VEH
WT THC
APP/PS1 THC
WT CBD
APP/PS1 CBD
WT THC+CBD
APP/PS1 THC+CBD

Figure 2

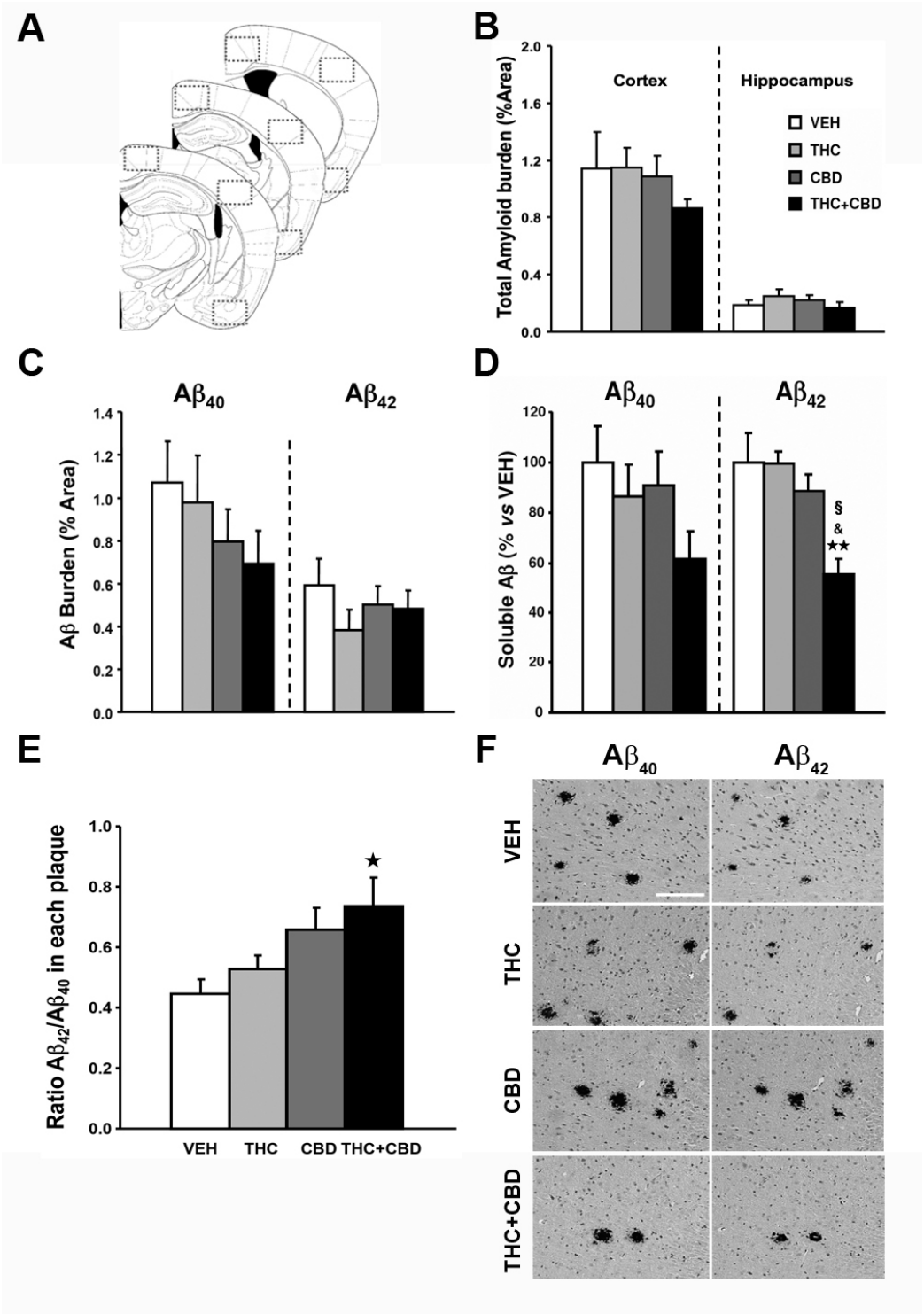
A
B
Cortex
Hippocampus
VEH
THC
CBD
THC+CBD
Total Amyloid burden (%Area)
C
Aβ40
Aβ42
Aβ Burden (% Area)
D
Soluble Aβ (% vs VEH)
§
&
★★
E
Ratio Aβ42/Aβ40 in each plaque
★
VEH
THC
CBD
THC+CBD
F
Aβ40
Aβ42
VEH
THC
CBD
THC+CBD

Figure 3

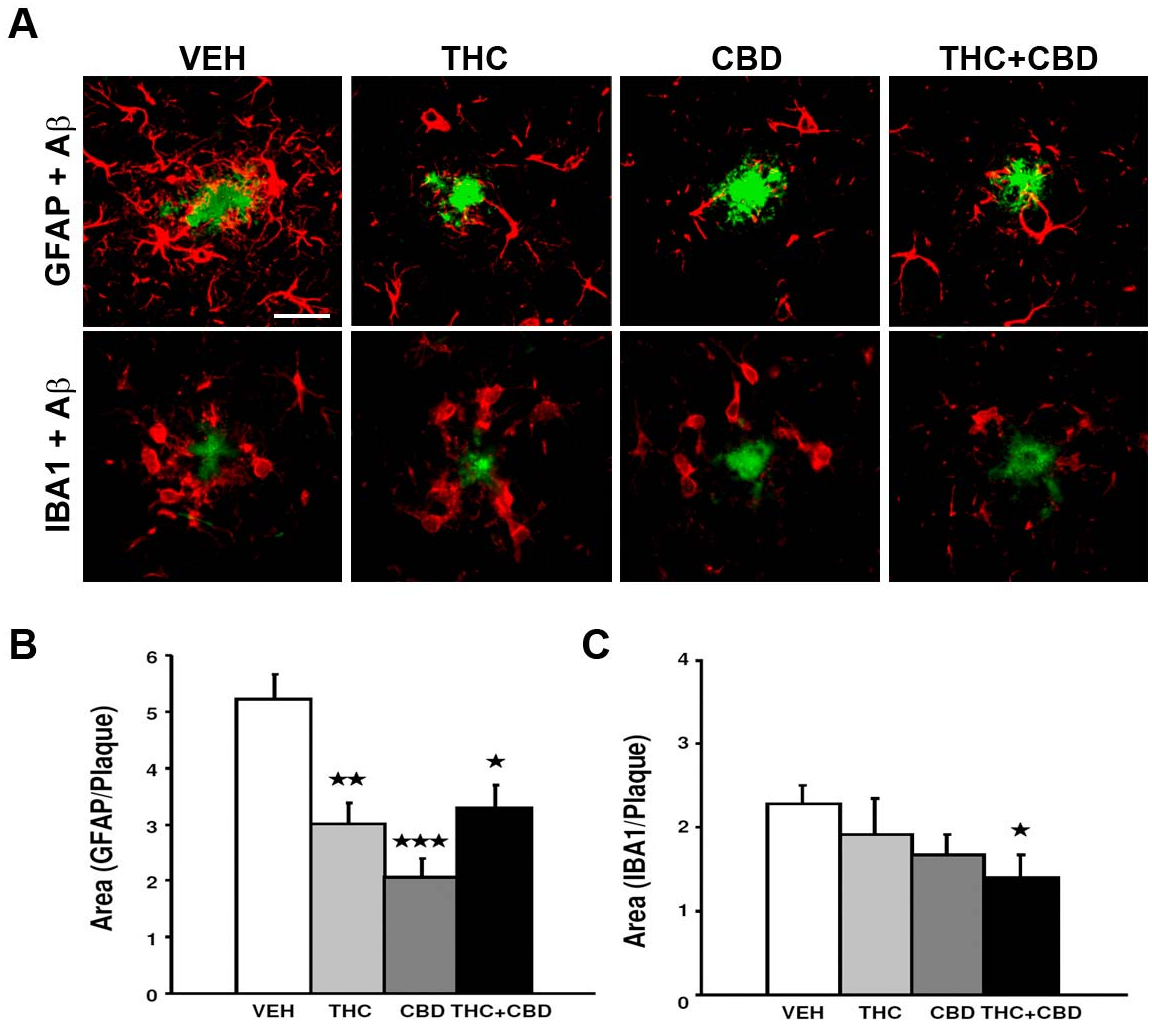
A
VEH
THC
CBD
THC+CBD
GFAP + Aβ
IBA1 + Aβ
B
Area (GFAP/Plaque)
0
1
2
3
4
5
6
VEH
THC
CBD
THC+CBD
C
Area (IBA1/Plaque)
0
1
2
3
4
VEH
THC
CBD
THC+CBD

Figure 4

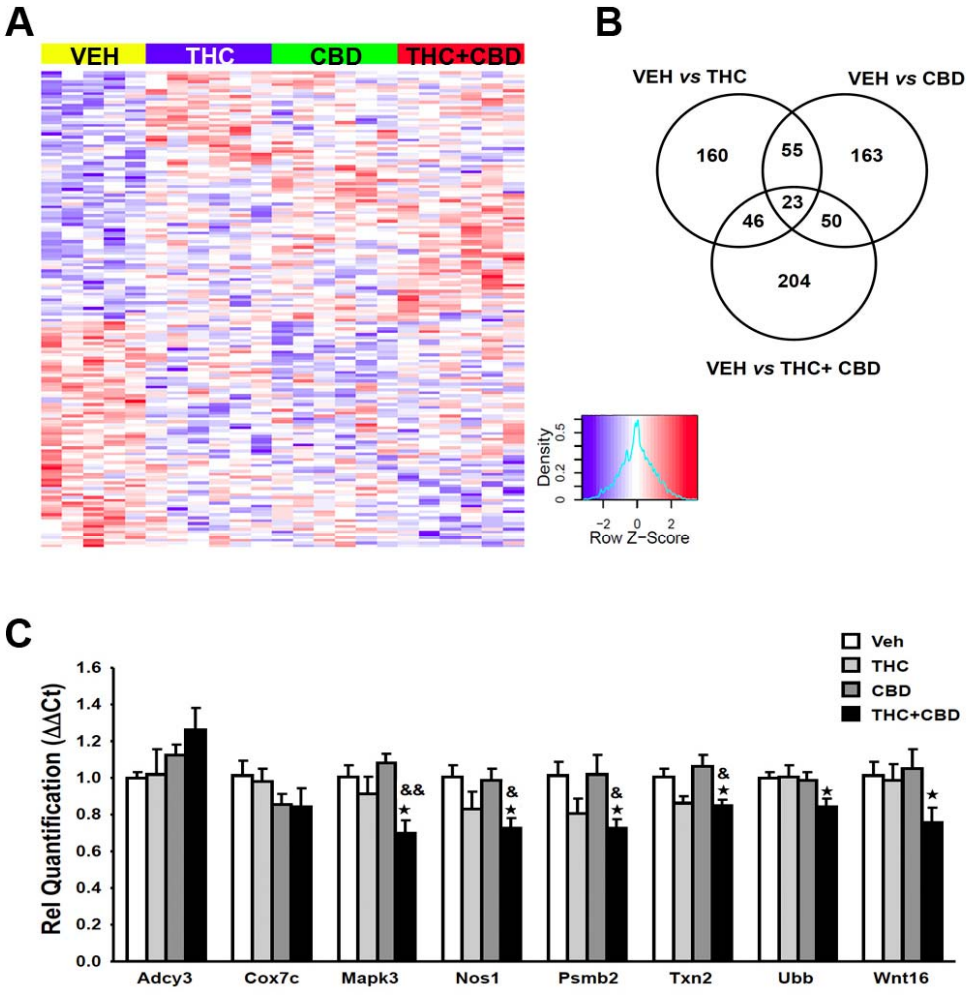
A
VEH
THC
CBD
THC+CBD
Density
0
0.2
0.5
−2
0
2
Row Z−Score
B
VEH vs THC
VEH vs CBD
160
55
163
23
46
50
204
VEH vs THC+ CBD
C
Veh
THC
CBD
THC+CBD
Rel Quantification (ΔΔCt)
0.0
0.2
0.4
0.6
0.8
1.0
1.2
1.4
1.6
Adcy3
Cox7c
Mapk3
Nos1
Psmb2
Txn2
Ubb
Wnt16

Figure 5

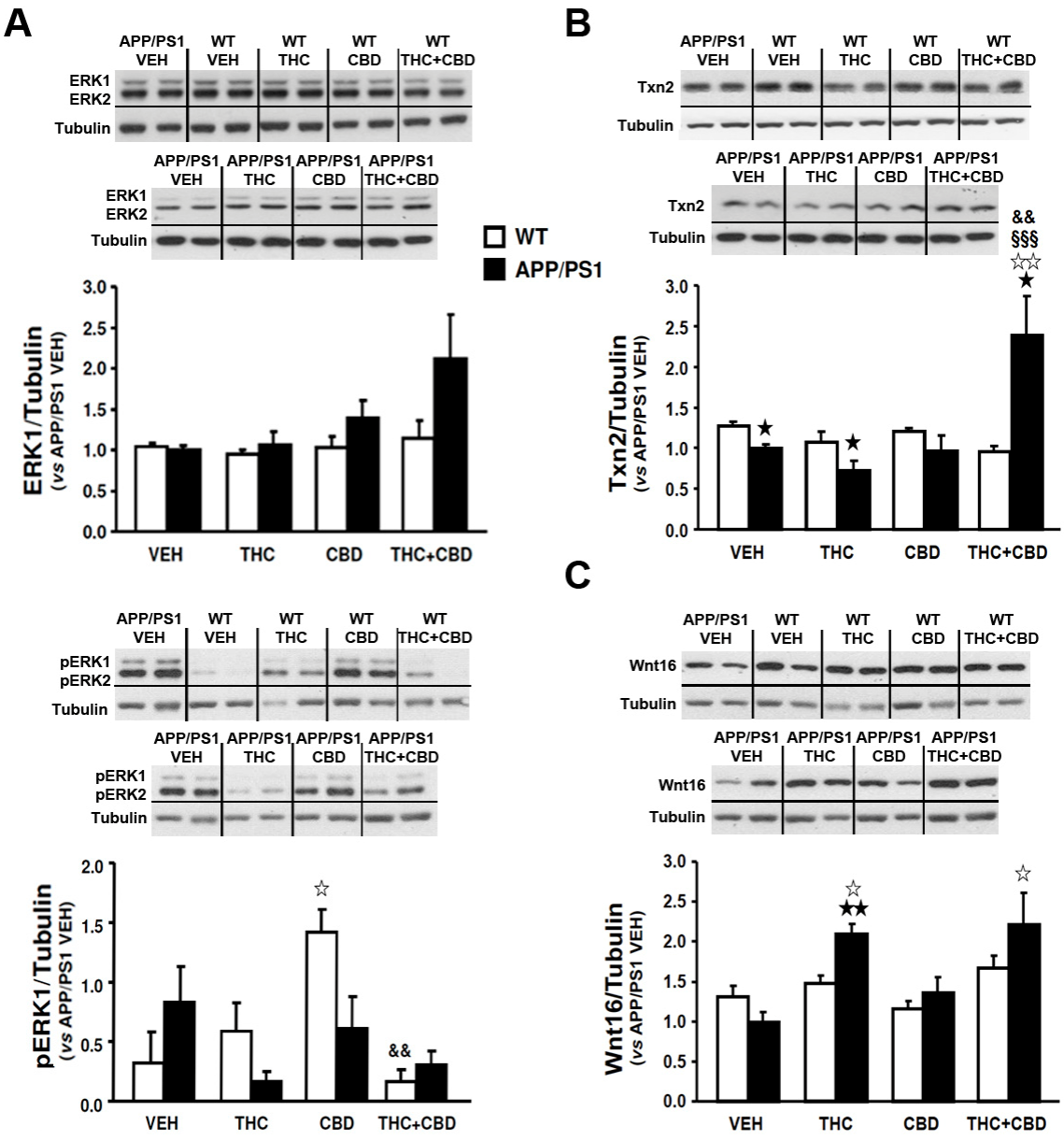
A
APP/PS1 VEH
WT VEH
WT THC
WT CBD
WT THC+CBD
ERK1
ERK2
Tubulin
APP/PS1 VEH
APP/PS1 THC
APP/PS1 CBD
APP/PS1 THC+CBD
ERK1/Tubulin (vs APP/PS1 VEH)
VEH
THC
CBD
THC+CBD
WT
APP/PS1
B
Txn2
Tubulin
&&
§§§
Txn2/Tubulin (vs APP/PS1 VEH)
C
pERK1
pERK2
pERK1/Tubulin (vs APP/PS1 VEH)
Wnt16
Wnt16/Tubulin (vs APP/PS1 VEH)